Published in final edited form as:
Biochemistry. 2011 June 7; 50(22): 4855–4866. doi:10.1021/bi200136e.

The Membrane Interface dictates Different Anchor Roles for "Inner Pair" and "Outer Pair" Tryptophan Indole Rings in Gramicidin A Channels

Hong Gu[1], **Kevin Lum**[2], **Jung H. Kim**[2], **Denise V. Greathouse**[1], **Olaf S. Andersen**[2,*], and **Roger E. Koeppe II**[1,*]

[1]Department of Chemistry and Biochemistry, University of Arkansas, Fayetteville, AR 72701

[2]Department of Physiology and Biophysics, Weill Cornell Medical College, New York, NY 10065

Abstract

We investigated the effects of substituting two of the four tryptophans (the "inner pair" $Trp^{9,11}$ or the "outer pair" $Trp^{13,15}$) in gramicidin A (gA) channels. The conformational preferences of the double-substituted gA analogues were assessed using circular dichroism spectroscopy and size-exclusion chromatography, which show that the inner tryptophans 9 and 11 are critical for the gA's conformational preference in lipid bilayer membranes. [$Phe^{13,15}$]gA largely retains the single-stranded helical channel structure, whereas of [$Phe^{9,11}$]gA exists primarily as double-stranded conformers. Within this context, the ^{2}H-NMR spectra from labeled tryptophans were used to examine the changes in average indole ring orientations, induced by the Phe substitutions and by the shift in conformational preference. Using a method for deuterium labeling of already synthesized gAs, we introduced deuterium selectively onto positions C2 and C5 of the remaining tryptophan indole rings in the substituted gA analogues for solid-state ^{2}H-NMR spectroscopy. The (least possible) changes in orientation and overall motion of each indole ring were estimated from the experimental spectra. Regardless of the mixture of backbone folds, the indole ring orientations observed in the analogues are similar to those found previously for gA channels. Both Phe-substituted analogues form single-stranded channels, as judged from the formation of heterodimeric channels with the native gA. [$Phe^{13,15}$]gA channels have Na^+ currents that are ~50% and lifetimes ~80% those of native gA channels. The double-stranded conformer(s) of [$Phe^{9,11}$]gA do not form detectable channels. The minor single-stranded population of [$Phe^{9,11}$]gA forms channels with Na^+ currents that are ~25% and single-channel lifetimes that are ~300% those of native gA channels. Our results suggest that Trp^9 and Trp^{11}, when "reaching" for the interface, tend to drive both monomer folding (to "open" a channel) and dimer dissociation (to "close" a channel). Furthermore, the dipoles of Trp^9 and Trp^{11} are relatively more important for the single-channel conductance than are the dipoles of Trp^{13} and Trp^{15}.

Keywords

tryptophan dipole; single-channel lifetime; solid-state NMR; deuterium

The physico-chemical principles underlying membrane protein structure and function remain a challenge due to the nature of biological membranes, being thin and heterogeneous in chemical composition. Yet, it is critical to understand how the amino acid sequence determines both the structural preference and function of membrane proteins. In this context

Address correspondence to: Roger E. Koeppe II, Tel. (479) 575-4976; Fax. (479) 575-4049; rk2@uark.edu; or Olaf S. Andersen, Tel. (212) 746-6350; Fax. (212) 746-8678; sparre@med.cornell.edu.

the gramicidin A (gA) channels play an important role because, though relatively small in size, they have very well defined properties. They thus are useful tools to study the principles that govern membrane protein structure and function.

An important feature of the gA channels is the presence of four tryptophan residues in each subunit. The subunit sequence is formyl-VGA<u>L</u>A<u>V</u>V<u>V</u>W^{9}<u>L</u>W^{11}<u>L</u>W^{13}<u>L</u>W^{15}-ethanolamide (D-residues underlined). In gA channels, tryptophan has several roles: The eight Trp side chains orient the dimeric channel (1). They stabilize the single-stranded dimeric conformation (2-6), and they promote cation transport through the channel through favorable ion-dipole interactions (7-12). These observations suggest that tryptophan may have important contributions to the folding and function of membrane proteins.

The unique side chain characteristics of Trp are believed to be important to membrane proteins in general. Trp is a large aromatic, amphiphilic amino acid with a dipole moment of ≈ 2 Debye along the C5→N1 axis (13). Substitutions of Trp by the more hydrophobic Phe have revealed important information about gA channels. For example, there is about a 2-fold decrease in the conductance of the channels formed by [Phe^{11}]gA, a natural product in the host organism *Bacillus brevis* (14, 15). Early studies showed that substitution of one, two (at positions 9 and 15 only), three or four Trps by Phe significantly decreases the gA channel conductance (7, 14, 16), and that this effect is not evenly distributed (7).

Recent evidence, based on analogues with 1-methylation of the indole ring nitrogen (17), has suggested that the influence of Trp 9 and 11 (designated the “inner pair” Trps) on gramicidin structure and function is rather different from the influence of Trp 13 and 15 (the “outer pair”). The detailed effects induced by the pairwise “double” Trp→Phe substitutions (“inner pair” Phe^{9,11}, or “outer pair” Phe^{13,15}) have not been investigated, however.

Recently, we developed a method for deuterium labeling of Trp indole ring positions 2 and 5 in intact gramicidins (18)(18). Here we apply the labeling method to the two remaining Trps in each of the doubly Phe-substituted gramicidins. The method allows us to report the consequences for the average ring orientations of the remaining tryptophans when a pair of Trps in a gramicidin subunit (“inner pair” or “outer pair”) is replaced by two phenylalanines. We also compare the properties of the channels formed by the “inner” and “outer” doubly substituted analogues with results from other Phe substitutions using single-channel electrophysiology (7), complemented by structural studies using CD spectroscopy, size-exclusion chromatography, and solid–state deuterium NMR spectroscopy. (The functional characterization of the four simultaneous Trp→Phe substitutions, in [Phe^{9,11,13,15}]gA, has been reported previously (3, 4, 19).)

Our results indicate that [Phe^{13,15}]gA folds predominantly into the single-stranded (SS) channel structure and that [Phe^{9,11}]gA folds predominantly into one of several possible (inert, or non-conducting) double-stranded (DS) structures, in agreement with an earlier characterization by SEC (20). Regardless of the folding preference, the Trp indole ring orientations change very little in [Phe^{9,11}]gA or [Phe^{13,15}]gA. The single-channel results show that the (SS) [Phe^{9,11}]gA channels have increased lifetimes, whereas the [Phe^{13,15}]gA channels, have decreased lifetimes, indicating that the analogues’ conformational preference is not a determinant of the SS channel lifetimes. Both pairs of Phe substitutions reduce the single-channel conductance, but the decrease is more pronounced when the inner Trp^{9,11} are removed to yield the [Phe^{9,11}]gA channels.

MATERIALS AND METHODS

Materials

Fmoc-Trp Wang resin and unlabeled Fmoc-protected amino acids were purchased from Advanced Chem Tech (Louisville, KY) and NovaBiochem (San Diego, CA). DMPC and DPhPC were from Avanti Polar Lipids (Alabaster, AL). Deuterated TFA (CF_3COOD), deuterium-depleted water, and D_2O were purchased from Cambridge Isotope Laboratories (Andover, MA). Methanol was from Burdick & Jackson (Muskegon, MI), and tetrahydrofuran from Waters, Inc. (Milford, MA). Regular filtered water was doubly deionized Milli-Q® water.

Peptide Synthesis

The Phe gramicidin analogues were synthesized on an Applied Biosystems 433A synthesizer using standard Fmoc-chemistry (21) and Trp Wang resin (Advanced Chem Tech, Louisville, KY). After the last synthesis step, peptides were finished by formylation: Following addition of 2.5 mL of DMF containing 80 mg *p*-nitrophenyl formate and 0.01 mL N-methyl-morpholine, the resin was stirred at 4 °C overnight. The resin was washed with DMF, and the peptide was cleaved from the resin with 20% ethanolamine in DMF at 25 °C for 48 hr (21). The peptide sequences are formyl-V^1-G-A-L-A-V-V^7-V-W-L-W-L-W-L-W^{15}-ethanolamine (D-residues underlined), but with Phe (F) substitution instead of Trp (W) at positions 9 and 11, or positions 13 and 15. The gramicidin analogue identity and purity were confirmed by electrospray ionization MS and reversed-phase HPLC (Zorbax SB80; 4.6 × 50 mm column of 3.5 μm octyl-silica, from MacMod analytical, Chadds Ford, PA).

Isotope Exchange

^{2}H exchange into the indole ring in gramicidin analogues—Deuterium was introduced on indole rings in existing peptides (post synthesis). In detail, 20 mg gramicidin analogue was weighed into a 4 mL glass vial equipped with a Teflon cap. Cold CF_3COOD (0.5 mL, pre-cooled on ice) was added to the vial with the gramicidin (all on ice). Because darkness is essential to prevent damage to the indole ring, the vial was covered with aluminum foil as quickly as possible. The solution was shaken in a cold room (4 °C) for 20 min. (Longer reaction times or higher temperatures cause damage to the peptide (22)). While the reaction is underway, it is essential to have 5 mL cold water ready in a centrifuge tube (polystyrene, 20 mL). Following the reaction, the TFA/gramicidin solution was transferred into the pre-cooled, water-containing tube to precipitate the deuterated gramicidin. After centrifugation in the cold (6000 rpm at 4 °C), the supernatant water was decanted. The deuterated gramicidin was washed three more times with water (using deuterium-depleted water for the last wash), followed by centrifugation. The resulting pellet was dried under vacuum (10^{-3} mm Hg). Finally, to remove final traces of residual TFA, the deuterated gramicidin was dissolved in 1 mL methanol and dried by vacuum centrifugation, twice.

Solid-state ^{2}H NMR spectroscopy

Oriented sample preparation—Aligned gramicidin/lipid samples were prepared using the procedure described by van der Wel et al. (23). Each sample consisted of four μmol gramicidin and 80 μmol DMPC to maintain a gramicidin/lipid molar ratio of 1:20. Gramicidin/lipid samples in chloroform/methanol were distributed evenly onto approximately 40 glass slides (4.8 × 23 × 0.07 mm). Samples were dried first under a stream of N_2 and then in vacuum, and then were hydrated using deuterium-depleted water to achieve 45% (w/w) overall hydration, which ensures fully hydrated bilayers (24). Before the NMR measurements, the samples were allowed to equilibrate at 40 °C for at least 72 hr in order to secure optimal alignment.

NMR measurements—To investigate the tryptophan conformations (25, 26), ^{2}H NMR spectra were recorded with the lipid bilayer normal aligned either parallel to the magnetic field (β=0°), or perpendicular (β=90°), using a Bruker AMX2 300 spectrometer, operating at 46 MHz for ^{2}H (27). Measurements were done at 50 °C, to maintain the lipids in the liquid-crystalline phase (28) and to optimize the detection of ^{2}H resonances (see also reference (26)). The ^{2}H measurements involved 3 to 5 million acquisitions and were done using a quadrupolar echo pulse sequence (29) with an echo delay of 125 μs, a 90° pulse duration of 3.3 μs, and a 60 ms interpulse time. A line broadening of 400 Hz was applied to the ^{2}H spectra. Phosphorus (^{31}P) NMR experiments were performed to check the alignment of the lipid bilayers (23).

Data analysis—^{2}H NMR spectra have been used to examine the average orientations of Trp indole rings in gA channels (5, 11, 25). Each deuterium nucleus produces two symmetric peaks, separated by their quadrupolar splitting. The quadrupolar splittings can be converted to orientation angles for the individual C-D bonds on the indole ring:

$$\Delta\nu_q = \frac{3}{2} S_{zz} \left(\frac{e^2 qQ}{h}\right) \left(\frac{1}{2}\left[3\cos^2\theta - 1\right]\right) \left(\frac{1}{2}\left[3\cos^2\beta - 1\right]\right).$$

In this equation, (e^2qQ/h) is the quadrupolar coupling constant (QCC), which for deuterons on aromatic rings has a measured static value of ~180 kHz (30). The “effective” quadrupolar coupling constant may be reduced by molecular motion (31), which is estimated by a principal order parameter S_{zz} between zero and one (25). Angle θ is the angle between a particular C-D bond and the membrane normal; angle β is the angle between the membrane normal and the magnetic field, either 0° or 90°. For gA channels, the helix axis also is aligned with the membrane normal (25, 32). Assignments of quadrupolar splittings to the C2-D and C5-D indole ring bonds were based upon the relative peak intensities and the known position-dependent kinetics for the indole ring isotope exchange (25). Changes in indole ring average orientation and dynamics were estimated by calculating the backbone-independent ring orientation angles ρ_1 and ρ_2 (Fig 1), as the “effective” quadrupolar coupling constant (QCC * S_{zz}) was searched, as described previously (25). In this method, the RMSD between observed and calculated quadrupolar splittings is calculated for all possible values of ρ_1 and ρ_2 for a particular S_{zz}; the reported ρ_1 and ρ_2 values for each S_{zz} are those for which the RMSD was least.

Circular dichroism spectroscopy and size-exclusion chromatography

Samples having a gramicidin:lipid ratio of 1:50 were prepared using salt-free DMPC as described in (33). UV absorbance at 280 nm, wherein ε = 5,210 $Trp^{-1}M^{-1}cm^{-1}$ (34), was used to determined the final gramicidin concentration in each sample. CD spectra were recorded at room temperature using a Jasco J710 CD spectrometer with 0.1 cm path length cell, 1.0 nm bandwidth; 0.2 nm step resolution and 50 nm/min scan speed. Each spectrum is an average of 6 scans.

The fractions of double-stranded (DS) and single-stranded (SS) conformers of each gA analogue were estimated using size-exclusion chromatography (SEC) in lipid suspensions (17, 20, 35). The gramicidin:lipid dispersions were injected into an Ultrastyrogel 1000 Å column (7 μM, 7.8×300 mm; mobile phase: 100% tetrahydrofuran at 1.0ml/min; Waters, Inc., Milford, MA), and the elution times for DS and SS conformers were recorded.

Single-Channel Measurements

Planar bilayers were formed from *n*-decane solutions (2.5% w/v) of DPhPC, across a hole (~1.6 mm diameter) in a Teflon® partition that separates two 1.0 M NaCl aqueous solutions at pH 7.0. Single-channel measurements were done at 25 ± 1 °C using the bilayer punch method (36), using pipettes with tip diameter ~30 μm and a Dagan 3900 patch clamp amplifier (Dagan Corp, Minneapolis, MN). The applied potential was ±200 mV, with the front (or *cis*) chamber being the electrical reference (at 0 mV) and the bilayer punch in the rear (or *trans*) chamber.

The gA analogues were added from stock dilutions, made up in either ethanol or DMSO, to the electrolyte solution on both sides of the bilayer. The final concentrations ~2 pM for gA and [Phe^{13,15}]gA and 20 pM for [Phe^{9,11}]gA. The aqueous solution was stirred for 60 s after peptide addition, and the final ethanol or DMSO concentration was less than 0.25%, a concentration that has no effect on channel properties (37). The current signal was filtered at 2 kHz, digitized at 20 kHz and digitally filtered at 500 Hz. Single-channel current transitions were detected on-line and analyzed as described previously (38-40). The transition amplitudes and lifetime distributions are based on independent measurements at each polarity. The lifetime histograms were transformed into survivor distributions, with average channel lifetimes (τ) determined by fitting a single exponential distribution ($N(t)/N(0) = \exp\{-t/\tau\}$, where $N(t)$ denotes the number of channels with a lifetime longer than time t) to each histogram (39).

In the heterodimer formation experiments we used two different protocols. Most experiments were done with symmetric addition of both gramicidins to both sides of the bilayer, at the same concentrations that were used when characterizing the individual compounds. The solutions were stirred (for 60 s), and the channel activity was recorded and analyzed as described above. In each experiment, we isolated three to ten “small” membranes using the bilayer punch; the distribution of single-channel current transition amplitudes was similar among the recordings done with the different small membranes. In the experiments where we probed the orientation of the heterodimeric channels with respect to the applied potential, we added the amino acid-substituted gA analogue to only the *cis* compartment and gA to only the *trans* compartment (again stirring for 60 s after adding the gramicidins) and recorded the single-channel activity at +200 and −200 mV.

RESULTS

Conformational preference

Because successive Trp → Phe (or Trp → 1-Me-Trp) substitutions increase the propensity for folding into DS conformations as opposed to the SS channel conformation (17, 20), even in lipid membrane environments, we tested the conformational preferences following Phe substitutions of the “inner” pair (Trp^{9,11}) or the “outer” pair (Trp^{13,15}). The CD spectrum of [Phe^{13,15}]gA (Fig 2D) shows positive ellipticity between 210-240 nm, but of lower intensity than observed for native gA (Fig 2E), suggestive of a mixture of SS and DS conformations. By contrast, the CD spectrum of [Phe^{9,11}]gA (Fig 2D) shows negative ellipticity between 210-240 nm, suggestive of predominantly DS conformations (33). These findings were confirmed by SE chromatography; in agreement with an earlier report (20), [Phe^{9,11}]gA (Fig 2A) is ~75% DS (as peak 1 dominates in the SE chromatograms), whereas [Phe^{13,15}]gA (Fig 2B) is ~75% SS (as peak 2 predominates in the SE chromatograms). (The later small peaks in the chromatograms are due to changes in refractive index when the lipids elute.) Based upon these comparisons, we deduce that the “*inner*” tryptophans 9 and 11 are of major importance for maintaining the cation-conducting, membrane-spanning SS channel

conformation. Even though the [Phe^{9,11}]gA population is ~75% DS, it is the minor SS population that comprises the cation-conducting channels (see below).

Single-channel properties

Each of the double-substituted Phe analogues forms channels in bilayer membranes of DPhPC (Figs 3 and 4). gA and [Phe^{13,15}]gA have comparable channel-forming potencies, meaning that we needed to add similar amounts in order to observe similar channel appearance rates; [Phe^{9,11}] gA had lower channel forming potency, as we needed to add ten-fold more of this analogue to observe the same channel appearance rates, suggesting that the [Phe^{9,11}] gA channels are formed by a minor conformer (generally consistent with the SEC results). Compared to native gA channels, the single-channel currents carried by Na^+ are reduced by about 50% when the outer tryptophans are replaced ([Phe^{13,15}]gA) and by about 75% when the inner tryptophans are replaced to give [Phe^{9,11}]gA (Table 1).

Both gA and each of the analogues form channels with a single predominant current transition amplitude. The single-channel current transitions observed with [Phe^{9,11}]gA as well as [Phe^{13,15}]gA have a narrow current distribution (Fig 4A) typical of a single conducting conformation (functional conformer), and the single-channel lifetime distributions are described by single exponential distributions (Fig. 4B). The [Phe^{9,11}]gA single-channel lifetime is longer (Fig 4B) than that of native gA channels, and comparable to that of [Phe^{9}]gA channels (7); see also Table 1. We therefore deduce that the conducting [Phe^{9,11}]gA conformer is the *minor* SS conformer, not the major DS conformer, observed in the CD and SEC experiments (Fig 2). Likewise the conducting conformer of [Phe^{13,15}]gA also is SS, with a single-channel lifetime that is slightly less than that of native gA and [Phe^{9,11}]gA channels (Fig 4B). Results for the present double-substituted Trp→Phe gA analogues are listed together with results for other analogues (from (7)) in Table 1. Our assignment of the conformation of the conducting channels is confirmed in heterodimer experiments (see below). For each of the double-substituted Phe gA analogues, the (presumably inert) DS conformers were not observable by single-channel recording methods. The trends in the single-channel lifetimes indicate that having Trps at positions 9 and 11 will tend to *decrease* the lifetime, whereas having Trps at positions 13 and 15 has little effect on the single-channel lifetime (relative to having Phe at these positions).

Deuterium NMR spectra

The deuterium isotope exchange method enabled us to estimate the Trp indole ring orientations using ^{2}H NMR spectroscopy. In Fig 5 we show the ^{2}H NMR spectra for isotope-exchanged samples of [Phe^{13,15}]gA and [Phe^{9,11}]gA in oriented DMPC bilayers. The taller two pairs of peaks in each spectrum represent signals from the fast-exchanging C2 deuterons (25) of the two remaining Trp rings in each gramicidin analogue. Each particular ring C2 assignment was deduced by assuming that the relative order of splittings would not change from the known assignments in gA (25). Additional pairs of medium-intensity peaks represent signals from the respective C5 deuterons, which display lower isotope enrichment due to slower exchange with deuterium during the sample preparation. The quadrupolar splittings and assignments for the major pairs of peaks are summarized in Table 2. For comparison, the quadrupolar splittings for the corresponding deuterons in native gA are also listed. The resonances from the C5 deuterons of Trp^{13} and Trp^{15} in native gA both exhibit a quadrupolar splitting of 205 kHz; the corresponding resonances in [Phe^{9,11}]gA are both near 211 kHz (Table 2).

The minor peaks in Fig 5 can be attributed to contributions from the significant amounts (~25%) of minor conformers, as well as small amounts of ^{2}H exchange at C6 ring positions (25). The presence of the minor peaks nevertheless does not interfere with the assignments

for the C2 and C5 deuterons of the respective major conformations, namely the SS channel-forming [Phe^{13,15}]gA, and the DS non-channel [Phe^{9,11}]gA.

Trp ring orientations and dynamics

Because the backbone conformation may change in response to the mutation (Fig 2), it is desirable to present the Trp side chain orientations without reference to the backbone (i.e., without using χ_1 and χ_2). Moreover, even if the fold of the major conformer is preserved (Fig 2B, D), the detailed backbone geometry may undergo small adjustments. It is therefore useful to describe the indole ring orientations using rotation angles ρ1 and ρ2 about axes normal to the ring bridge (Fig 1). As a check on the ring dynamics, we calculated lowest RMSD and the variation of the best-fit values for the ρ1 and ρ2 angles as functions of the "apparent" QCC_{eff} (S_{zz}*QCC) value from 120 to 190 kHz for each of the Trp indole rings (25). These results are summarized in Fig 6, for which the ρ1 and ρ2 angles were allowed to vary independently, with neither ρ1 nor ρ2 held fixed in any of the calculations. Although only two data points (C2 and C5) were available for each ring, it is possible to exclude values of QCC_{eff} below about 135 kHz (Fig 6). Values in the range 135-180 kHz represent a principal ring order parameter S_{zz} between 0.75-1.0, although S_{zz} should not exceed the value of about 0.92 established for the gA backbone (25, 31). We conclude that the values of S_{zz} for the indole side chains of the remaining Trps in the major backbone conformers of [Phe^{13,15}]gA and [Phe^{9,11}]gA fall within a range of about 0.75-0.9.

For [Phe^{13,15}]gA—which largely retains the SS channel conformation (Fig 2)—the ring orientation angle ρ1 is not very sensitive to S_{zz} (Fig 6A, B). For S_{zz} assigned anywhere between 0.7 and 0.9 (QCC_{eff} from 130-160 kHz), ρ1 is about 36° for Trp^{9} and about 42° for Trp ^{11} in [Phe^{13,15}]gA. These results should be compared to the similar respective ρ1 values of ~37° and 46° in native gA (32). Also for the Trps in [Phe^{9,11}]gA, regardless of the DS conformation(s) now being dominant (Fig 2), the indole ring orientations remain similar to those in gA (25). The ρ1 values for Trp^{13} and Trp^{15} nevertheless become somewhat more sensitive to the choice of S_{zz} (Fig 6C, D). With only two data points—C2 and C5—for each ring, it is not feasible to unambiguously determine S_{zz}, so one is left with a range of 50°-55° for ρ1 of each Trp in [Phe^{9,11}]gA.

The values of ρ2 for Trps in both [Phe^{9,11}]gA and [Phe^{13,15}]gA show similar behavior and rather steep dependence upon the exact value of QCC_{eff} (S_{zz}; Fig 6). For [Phe^{13,15}]gA (Fig 6A, B), ρ2 varies from ~15° to ~30° over the range of QCC_{eff} between 140-170 kHz. For [Phe^{9,11}]gA, the ρ2 dependence on QCC_{eff} is steeper, varying from ~0° to ~35° over a range of QCC_{eff} between 140-170 kHz (Fig 6C, D). Again with only two data points for each Trp ring, we are not able to define exact values for S_{zz} or ρ2. Nevertheless, for similar ranges of S_{zz}, the trends for ρ2 as well as ρ1 correlate with previous findings for the parent gA dimer (25).

Heterodimer formation (test for structural equivalence)

Because the double Trp→Phe-substituted gA analogues display both SS and DS conformers (Fig. 2), we used a heterodimer formation assay (39), based on channel formation with native SS gA subunits, to establish the conformational identities of the conducting channels formed by the Trp→Phe-substituted gA analogues(41). In these experiments, native gA subunits are added together with either [Phe^{9,11}]gA or [Phe^{13,15}]gA subunits to both sides of the lipid bilayer. In such experiments, we observe four channel types (Fig. 7): the native gA and mutant [Phe^{13,15}]gA or [Phe^{13,15}]gA homodimeric channels, as well as two new channel types with properties that are intermediate to those of the symmetric, homodimeric channels. These new channels are heterodimeric (hybrid) channels formed by one gA and one [Phe^{9,11}]gA or [Phe^{13,15}]gA subunit. The heterodimers can occur in two orientations with

respect to the applied potential, gA/[Phe^{x,y}]gA and [Phe^{x,y}]gA/gA, where x and y denote the positions of the Trp→Phe substitutions, depending on whether the current moves from the gA subunit to the [Phe^{x,y}]gA subunit, or vice versa. The heterodimeric channels therefore often exhibit a split peak in a current transition amplitude histogram (4, 42, 43), as is the case here. That the hybrid channel conductance is orientation-dependent shows that cations experience an asymmetric barrier when traversing the transmembrane channel. The conductances of the heterodimeric channels, relative to the homodimeric parent channels, can be understood using a simple model in which the Trp→Phe substitution alters primarily the height of the central barrier that has to be traversed by the permeating ions and each subunit's contribution to the change in central barrier is independent of the identify of the other subunit. In this case, one would expect that the geometric mean of the conductances of the heterodimeric channels $\sqrt{g_{AB} \cdot g_{BA}}$ should be equal to the geometric mean of the conductances of the homodimeric channels $\sqrt{g_{AA} \cdot g_{BB}}$, where g_{XY} corresponds to the conductance of channels with that subunit composition (and A denoting gA and B the Trp→Phe substituted analogue). That is the case: for the [Phe^{9,11}] gA/gA heterodimers, $\sqrt{g_{AB} \cdot g_{BA}} / \sqrt{g_{AA} \cdot g_{BB}} = 1.04 \pm 0.01$ (mean ± S.D.); for the [Phe^{13,15}]gA/gA heterodimers, $\sqrt{g_{AB} \cdot g_{BA}} / \sqrt{g_{AA} \cdot g_{BB}} = 1.02 \pm 0.02$.

The relative appearance rates of homodimer and heterodimer events in the same lipid bilayer membrane serves as a sensitive test of subunit structural equivalence (39). The reason is that mutually compatible SS partner subunits that display the same backbone fold will form dimers at relative frequencies of appearance that are statistically predictable. (If the subunit fold in the heterodimers differed from that in the homodimers, there would be an energetic penalty for forming heterodimeric channels relative to the homodimeric parent channels.) In the experiments with the double-substituted Trp→Phe analogues, the observed numbers of heterodimeric channels, relative to the symmetric homodimeric channels, conform to the pattern observed earlier for independent subunit association without an energy barrier for refolding (39, 41), namely that the relative number of heterodimeric channels (Rn_H), given by

$$Rn_H = \sqrt{\frac{n_{AB} \cdot n_{BA}}{n_{AA} \cdot n_{BB}}}, \quad (1)$$

where n_{XY} corresponds to the number of appearances of channels with that subunit composition, is close to 1.0. (Because all the n_{XY}s are determined in the same experiment, in the same membrane over the same time interval, Rn_H is equal to the relative appearance rate for the hybrid channels (39, 41).) For the [Phe^{9,11}]gA/gA combination, $Rn_H \approx 1.02$; for the [Phe^{13,15}]gA/gA combination, $Rn_H \approx 0.73$. In either case, there are few if any subunit-specific interactions; cf. (39), such that we conclude that there is structural equivalence among the channel-forming subunits.

The respective heterodimer orientations that underlie the two hybrid channel peaks in the current transition amplitude histograms can be established in experiments where one analogue is added to only one side of a bilayer, and the other analogue to the other side (4). In such experiments, we observed shifts in the distribution of transitions in the heterodimer peaks, reflecting that the magnitude of the current through the heterodimeric channels varies with the polarity of the applied potential (Fig 8). In the [Phe^{13,15}]gA/gA experiments, we observed two peaks, one peak (at ~1.7 pA) representing symmetric [Phe^{13,15}]gA channels, and another peak representing the [Phe^{13,15}]gA/gA heterodimers. At −200 mV (when the current flow is from the [Phe^{13,15}]gA to the gA subunit) the heterodimer peak is at ~2.1 pA; at +200 mV (when the current flow is from the gA to the [Phe^{13,15}]gA subunit) the

heterodimer peak is at ~2.4 pA. That is, the current flow in the gA→[Phe^{13,15}]gA direction is greater than the current flow in the reverse direction (Fig. 8A). In the [Phe^{9,11}]gA/gA experiments, we observed only one peak, representing the [Phe^{9,11}]gA/gA heterodimers. At −200 mV (when the current flow is from the [Phe^{9,11}]gA to the gA subunit) the heterodimer peak is at ~1.6 pA; at +200 mV (when the current flow is from the gA to the [Phe^{9,11}]gA subunit) the heterodimer peak is at ~1.8 pA. Again, the current flow in the gA→gA[Phe^{9,11}] direction is greater than the current flow in the [Phe^{9,11}]gA→gA direction (Fig. 8B).

With the respective channel orientations known (Fig. 8), is becomes possible to assign the single-channel current magnitude and lifetime for each of the heterodimeric channels in both orientations. Not only the single-channel current transitions, but also the single-channel lifetimes vary as a function of the orientation of the heterodimeric channels with respect to the applied potential (Table 3). Though the difference is small compared to the experiment-to-experiment variation, the relative difference determined in individual experiments; $(\tau_{AB} - \tau_{BA})/\sqrt{\tau_{AA} \cdot \tau_{BB}}$, where τ_{XY} corresponds to the lifetime of the channels with the XY subunit composition, is different from zero—being 0.14 ± 0.05 (mean ± range) for the [Phe^{9,11}]gA/gA and 0.10 ± 0.02 for the [Phe^{13,15}]gA/gA heterodimers. As was the case for the channel appearances, the single-channel lifetimes of the heterodimeric channels, relative to the symmetric homodimeric channels, conform to the statistically predictable pattern observed earlier (39, 41), namely that the relative heterodimer lifetime ($R\tau_H$), given by

$$R\tau_H = \sqrt{\frac{\tau_{AB} \cdot \tau_{BA}}{\tau_{AA} \cdot \tau_{BB}}} \quad (2)$$

is close to 1.0. For the [Phe^{9,11}]gA/gA combination, $R\tau_H \approx 1.03$; for the [Phe^{13,15}]gA/gA combination, $R\tau_{Hr} \approx 0.96$. In either case there is little if any subunit-specific strain at the subunit interface, cf. (39).

DISCUSSION

We report on the use of a method for deuterium labeling of Trp indole rings in already existing peptides to explore the consequences of double Trp→Phe mutations in gramicidin A (gA) channels. In separate experiments, the inner pair and then the outer pair of anchoring Trp residues were “mutated” to Phe, by means of chemical synthesis. By using the method for deuterium labeling of already existing peptides, we were able to introduce deuterium onto the peptide-incorporated indole rings selectively, at positions C2 and C5 of each tryptophan, for use in solid-state ^{2}H-NMR experiments. The Trp→Phe substitutions alter the gA analogues’ conformational preference. Using a backbone-independent analysis (25), the assigned spectra from two different labeled Trps in each double Phe-substituted gA analogue were used to examine the changes in average indole ring orientations induced by the Phe substitutions. In turn, we will discuss the backbone folding preferences, average indole ring orientations and conducting channel structure and function, as revealed by the single-channel conductances and lifetimes.

Folding preference of double Phe gA analogues

The conformational consequences of the double Trp→Phe substitutions were examined using CD spectroscopy and SE chromatography. Generally, it is known that there are two general classes of folding patterns for gA, resulting in two different types of conformations. One conformational class is the (right-handed) head-to-head, SS $\beta^{6.3}$-helix, which functions as a cation-conducting channel (45, 46). The other conformational class is a family of DS intertwined double helices (47-50).

The CD spectra of the double Phe-substituted gramicidin analogues in DMPC vesicles are dominated by these two different patterns of folding. The spectrum of [Phe^{13,15}]gA is similar to that of native gA in DMPC bilayers (Figure 2), indicating that [Phe^{13,15}]gA adopts predominantly the SS β$^{6.3}$-helical channel conformation. The spectrum of [Phe^{9,11}]gA is quite different, suggesting that the analogue adopts predominantly a DS non-conducting conformation. The CD spectra of the double Phe-substituted gramicidin analogues thus suggest different effects on the peptide secondary structure preference in lipid bilayers based upon the different positions of Trp indole side chains.

The results from size-exclusion chromatography (SEC) agree with the conclusions from the CD spectra. For [Phe^{13,15}]gA, about 75% of this analogue elutes from the SEC column as monomers. The most likely interpretation of the SEC elution profile is that 75% of [Phe^{13,15}]gA remains in the SS β$^{6.3}$-helical channel structure in lipid bilayers. The SS conformation of [Phe^{13,15}]gA (but not of [Phe^{9,11}]gA) therefore is expected to dominate the NMR spectra. In contrast, the SEC elution profile of [Phe^{9,11}]gA in DMPC shows that the majority of this analogue elutes as DS dimers, suggesting that this peptide prefers a DS conformation rather than the SS channel structure in DMPC. The SEC results thus support the conclusion from the CD analysis that substitution of the inner, more buried, Trps at positions 9 and 11 significantly shifts the gramicidin A structure away from the SS channel conformation toward the DS dimer conformation. Qualitatively similar results were reported by Salom et al. (20). These changes in conformational preference reflect primarily the removal of the indole NH, not the introduction of the Phe, as a similar shift in conformational preference was observed when Trp was replaced by N-methyl-Trp (17).

In general, the energetic cost to bury the four Trps within the lipid bilayer makes it unfavorable for native gA to remain folded in the DS non-conducting conformation (3). Phe like Trp is an aromatic amino acid, but is less polar and lacks hydrogen-bonding ability, whereas Trp is amphipathic and able to be a hydrogen-bond donor by means of the indole NH group. Trp furthermore has a dipole moment of ≈ 2 Debye along the C5→N1 axis (13). The observed conformational shift thus may be due to these differences between the Trp and Phe side chain characteristics, with the hydrogen bond formation likely to be dominant (17). Due to the loss of H-bonding ability, the Phe ring can be buried more deeply than the Trp ring, which becomes important because the DS conformations will bury side chains 9 and 11 essentially near the bilayer center. It therefore should not be surprising that Trp→Phe substitutions at positions 9 and 11 (but less so at positions 13 and 15) enable a conformational shift from SS toward DS gramicidin conformers.

Effect of double Phe substitution on remaining Trp indole ring orientations

For the analysis of Trp indole ring orientations, two labels (C2 and C5) are available for each Trp ring. The assignments of observed quadrupolar splittings to ring positions C2 and C5 are unambiguous, based upon the distinct and strong correlation between the rate of ^{2}H chemical exchange (during sample preparation) and the intensities of the subsequently observed ^{2}H NMR peaks, in the order: C2 ≫ C5 ≫ (other ring positions) (25). The changes in the C2-D and C5-D quadrupolar splitting for each ring indicate that the Trp indole rings in gA did undergo modest changes in their orientations upon replacement of two nearby Trps with Phe. With the ring position (C2 and C5) peak assignments known, we adopted a “minimalist” approach and used the principle of “least change,” thereby assigning each set of two quadrupolar splittings (having comparable intensities within the set) to the remaining Trps in the sequence, such that the overall assignments for the set were most similar to the known quadrupolar splitting assignments (25) for the native gA channel.

Comparing the orientations for each indole ring in [Phe^{9,11}]gA and [Phe^{13,15}]gA, one finds that the acceptable ranges of ρ1 and ρ2, for example ρ1 values of about 36°-42° for Trp^{9} and

Trp[11], are similar to those observed for the gA channel itself (25), suggesting that the orientation of any Trp residue is not much altered by Trp→Phe substitutions at other positions or by the change of backbone conformation. It appears, therefore, that the observed indole ring orientations are probably determined more by the properties of the membrane/water interface than by the backbone conformation. The trends in ρ2 (Figure 6) are more dependent upon the assumed value of S_{zz}, which is not accurately determined from the available data. The qualitative differences between the "inner pair" as compared to the "outer pair" indole ring behavior (Figure 6) are preserved from gA itself (25).

Single-channel Properties

In contrast to the NMR experiments, as demonstrated by the heterodimer experiments, the single-channel experiments report exclusively on the properties of the SS conformation, for both [Phe[13,15]]gA (where it is the major conformer) and [Phe[9,11]]gA (where it is the minor conformer). Consistent with the [Phe[9,11]]gA channels being formed by the minor conformer, we needed to add ten-fold higher concentrations of [Phe[9,11]]gA than of [Phe[13,15]]gA or gA to observe equivalent numbers of channel events. That the fold of the channel-forming subunits is similar can be deduced by calculating the energetic cost of forming the heterodimeric channels, relative to the homodimeric channels ($\Delta\Delta G^0$), which is estimated as (40, 41):

$$\Delta\Delta G^0=\Delta G^0_{\mathrm{H}} - \frac{\Delta G^0_{\mathrm{AA}}+\Delta G^0_{\mathrm{BB}}}{2} = -\frac{k_{\mathrm{B}}T}{2}\ln\{Rn_{\mathrm{H}}\cdot R\tau_{\mathrm{H}}\}, \quad (3)$$

where ΔG^0_{H}, ΔG^0_{AA} and ΔG^0_{BB} denote the free energy of forming heterodimers and the symmetric homodimers, respectively, k_{B} is Boltzmann's constant and T is temperature in kelvin. Using the values for Rn_{H} and $R\tau_{\mathrm{H}}$ reported in Fig 7, $\Delta\Delta G^0$ is within 1 kJ/mol of zero. We conclude that the conformers of [Phe[9,11]]gA and [Phe[13,15]]gA that assemble to form the conducting channels are structurally equivalent to the channels with SS subunits formed by the native gA. In terms of channel function, therefore, the observed differences in the single-channel conductances and lifetimes reflect the consequences of the different Trp indole ring positions within the context of a fixed backbone conformation for these "inner" and "outer" sequence isomers.

When the outer Trp[13] and Trp[15] are removed, the effects are modest (Table 1): the single-channel conductance is about 50% lower, and the lifetime is reduced by 10 – 20%. These results are expected because each of the four Trps enhances the cation flow through native gA channels (7) due to favorable ion-dipole interactions that lower the energy barrier for crossing the channel center (9, 10), and the outer Trps interact favorably with water and/or polar groups at the membrane/water interface and stabilize the SS dimeric transmembrane channel.

The changes in channel properties are more dramatic when the inner Trp[9] and Trp[11] are removed. The observed increase in the lifetime, together with the decreased conductance, serves to emphasize that the single-channel conductance and lifetime are independent properties, extending previous conclusions (7, 51). The single channel conductance for [Phe[9,11]]gA is about 25% that of native gA channels, thus illustrating the importance of the inner Trp[9] and Trp[11] residues for the cation conductance. The larger changes in the single-channel conductance, relative to the [Phe[13,15]]gA channels, reflect in part that the Trp[9] and Trp[11] side chain dipoles are closer to the channel center. Trp[9] and Trp[11] therefore would be expected to have larger effects on the energy barrier for ion movement through the pore, consistent with previous kinetic analyses (44, 52), which showed that Trp[9] has a large effect

on the rate constant for crossing the central barrier (44) and that replacing all four Trps (in [Phe^{9,11,13,15}]gA, also known as gramicidin M) also causes large changes in the rate constant for crossing the central barrier (52). Trp→Phe substitutions also alter the kinetics of ion entry/exit (44, 52). At the same time, the transmembrane dimers show three-fold longer lifetimes (Table 1) when Trp^{9} and Trp^{11} are absent. Interestingly, a dramatically short lifetime of 5 ms is observed for the triply substituted [Phe^{9,13,15}]gA (7), namely when only Trp^{11} is present. It is evident that Trp^{11} destabilizes the transmembrane dimer whereas Trp^{13} and Trp^{15} serve to increase the lifetimes of the conducting dimers. Trp^{9} often contributes a mild stabilization, although its detailed influence on the single-channel lifetime depends upon the context of which other tryptophans are present.

The properties of the heterodimeric channels add to this picture. Because each of the analogue subunits combines readily with a native gA SS subunit, with little if any strain at the subunit interface, all of the conducting channels indeed are formed by SS $\beta^{6.3}$-helical subunits.

The heterodimer experiments also provide insight into the conductance changes caused by Trp→Phe substitutions. The geometric mean of the single-channel conductances of the hybrid channels is equal to the geometric mean of the conductances of the symmetric parent channels, with the ratio $\sqrt{(g_{AB} \cdot g_{BA}) / (g_{AA} \cdot g_{BB})}$ being close to 1 (1.04 fo the [Phe^{9,11}]gA/gA pair and 1.02 for the [Phe^{13,15}]gA/gA pair). This result suggests that the Trp→Phe substitutions in each subunit have independent effects on the energy barrier for crossing the channel center, meaning that the peak height of the energy barrier in the heterodimers is the algebraic mean of the peak height in the homodimers. The situation is more complicated, however, as evident from the split in the peaks representing the hybrid channels in the current transition amplitude histograms (Figs. 7 and 8). This asymmetry shows, as expected, that the energy barrier that the ions have to surmount in order to move through the channel is asymmetric in the heterodimeric channels. The asymmetry in the peaks representing the heterodimers, defined as $(g_{AB} - g_{BA}) / \sqrt{g_{AA} \cdot g_{BB}}$, is similar in magnitude (between 0.12 and 0.13) for the [Phe^{9,11}]gA/gA and [Phe^{13,15}]gA/gA heterodimers even though the Trp^{9,11} pair is closer to the channel center than the Trp^{13,15} pair.

We finally note that we observed only symmetric [Phe^{13,15}]gA, not [Phe^{9,11}]gA, channels when the gA analogues were added to only one side of the bilayer. (We did not observe symmetric gA channels after asymmetric addition to only one side of the bilayer, consistent with previous observations (2).) The different behavior of [Phe^{13,15}]gA could reflect its conformational preferences. One would expect that the DS conformers could insert and span the bilayer. If the DS conformers are the preferred conformers, then they may not readily dissociate but rather remain as bilayer-spanning entities, which would account for why we did not observe many symmetric SS [Phe^{9,11}]gA channels. If, however, the DS conformers are not preferred, they could dissociate following insertion and fold into SS conformers at both interfaces, which would account for the observation of symmetric, SS [Phe^{13,15}]gA channels after asymmetric addition of the analogue. Further details of these phenomena are under investigation.

Summary and Conclusions

The average indole ring orientations and overall motion of Trp rings in double Phe substituted gA analogues ([Phe$^{13, 15}$] gA, and [Phe$^{9, 11}$]gA) were defined by experimental ^{2}H-NMR spectra. Backbone conformations were monitored by CD spectroscopy and size-exclusion chromatography. The results show that the substitution of two Trps in a gramicidin subunit by Phe may alter the backbone conformation of lipid membrane-incorporated gramicidin, depending upon the positions of the substitutions. The

Phe^{13,15} gA analogue adopts predominantly the single-stranded β$^{6.3}$-helical channel conformation, whereas the Phe^{9,11} gA analogue adopts predominantly a double-stranded non-conducting conformation. The Phe substitutions alter only slightly the average orientations of the remaining tryptophans, based on only modest changes in the observed indole ring ^{2}H quadrupolar splittings in response to the Phe substitutions. For both analogues, the cation-conducting channels are single-stranded β$^{6.3}$-helical dimers, and the single-channel results reveal that the dipoles of Trp^9 and Trp^{11} are relatively more important for the cation conductance than are the dipoles of Trp^{13} and Trp^{15}.

Acknowledgments

This work was supported in part by NIH grants GM70971, GM21342, RR15569 and RR31154; and by the Arkansas Biosciences Institute.

References

1. Ketchem RR, Hu W, Cross TA. High-resolution of gramicidin A in a lipid bilayer by solid-state NMR. Science. 1993; 261:1457–1460. [PubMed: 7690158]
2. O'Connell AM, Koeppe RE II, Andersen OS. Kinetics of gramicidin channel formation in lipid bilayers: transmembrane monomer association. Science. 1990; 250:1256–1259. [PubMed: 1700867]
3. Durkin JT, Providence LL, Koeppe RE II, Andersen OS. Formation of non-β$^{6.3}$-helical gramicidin channels between sequence-substituted gramicidin analogues. Biophys J. 1992; 62:145–159. [PubMed: 1376164]
4. Fonseca V, Daumas P, Ranjalahy Rasoloarijao L, Heitz F, Lazaro R, Trudelle Y, Andersen OS. Gramicidin channels that have no tryptophan residues. Biochemistry. 1992; 31:5340–5350. [PubMed: 1376621]
5. Hu W, Lee KC, Cross TA. Tryptophans in Membrane proteins: Indole ring orientations and functional implications in the gramicidin channel. Biochemistry. 1993; 32:7035–7047. [PubMed: 7687467]
6. Arumugam S, Pascal S, North CL, Hu W, Lee KC, Cotten M, Ketchem RR, Xu M, Brenneman M, Kovacs F, Tian F, Wang A, Huo S, Cross TA. Conformational trapping in a membrane environment: A regulatory mechanism for protein activity? Proc Natl Acad Sci USA. 1996; 93:5872–5876. [PubMed: 8650185]
7. Becker MD, Greathouse DV, Koeppe RE II, Andersen OS. Amino acid sequence modulation of gramicidin channel function: effects of tryptophan-to-phenylalanine substitutions on the single-channel conductance and duration. Biochemistry. 1991; 30:8830–8839. [PubMed: 1716152]
8. Hu W, Cross TA. Tryptophan hydrogen bonding and electric dipole moments: Functional roles in the gramicidin channel and implications for membrane proteins. Biochemistry. 1995; 34:14147–14155. [PubMed: 7578012]
9. Andersen OS, Greathouse DV, Providence LL, Becker MD, Koeppe RE II. Importance of tryptophan dipoles for protein function: 5-fluorination of tryptophans in gramicidin A channels. J Am Chem Soc. 1998; 120:5142–5146.
10. Dorigo AE, Anderson DG, Busath DD. Noncontact dipole effects on channel permeation. II. Trp conformations and dipole potentials in gramicidin A. Biophys J. 1999; 76:1897–1908. [PubMed: 10096887]
11. Cotten M, Tian C, Busath DD, Shirts RB, Cross TA. Modulating dipoles for structure-function correlations in the gramicidin A channel. Biochemistry. 1999; 38:9185–9197. [PubMed: 10413493]
12. Cole CD, Frost AS, Thompson N, Cotten M, Cross TA, Busath DD. Noncontact dipole effects on channel permeation. VI. 5F- and 6F-Trp gramicidin channel currents. Biophys J. 2002; 83:1974–1986. [PubMed: 12324416]
13. Weiler-Feilchenfeld HA, Pullman A, Berthod H, Giessner-Trettre C. Experimental and quantum-chemical studies of the dipole moments of quinoline and indole. J Mol Struct. 1970; 6:297–304.

14. Bamberg E, Noda K, Gross E, Läuger P. Single-channel parameters of gramicidin A, B, and C. Biochim Biophys Acta. 1976; 419:223–228. [PubMed: 55275]
15. Sawyer DB, Williams LP, Whaley WL, Koeppe RE II, Andersen OS. Gramicidins A, B, and C form structurally equivalent ion channels. Biophys J. 1990; 58:1207–1212. [PubMed: 1705449]
16. Heitz F, Spach G, Trudelle Y. Single channels of 9, 11, 13, 15-destryptophyl-phenylalanyl-gramicidin A. Biophys J. 1982; 40:87–89. [PubMed: 6182929]
17. Sun H, Greathouse DV, Andersen OS, Koeppe RE II. The preference of tryptophan for membrane interfaces: Insights from N-methylation of tryptophans in gramicidin channels. J Biol Chem. 2008; 283:22233–22243. [PubMed: 18550546]
18. Gu H, Thomas G, Subotic A, Liyanage R, Lay J, Koeppe RE 2, Greathouse DG. *In situ* deuteration of Trp indole rings in peptides. Biophys J. 2005; 88:141a. abstract.
19. Heitz F, Gavach C, Spach G, Trudelle Y. Analysis of the ion transfer through the channel of 9,11,13,15-phenylalanylgramicidin A. Biophys Chem. 1986; 24:143–148. [PubMed: 2428416]
20. Salom D, Pérez-Payá E, Pascal J, Abad C. Environment- and sequence-dependent modulation of the double-stranded to single-stranded conformational transition of gramicidin A in membranes. Biochemistry. 1998; 37:14279–14291. [PubMed: 9760266]
21. Greathouse DV, Koeppe RE II, Providence LL, Shobana S, Andersen OS. Design and characterization of gramicidin channels. Methods in Enzymol. 1999; 294:525–550. [PubMed: 9916247]
22. Gu, H. Ph D Thesis. University of Arkansas; 2008. Application of tryptophan derivatives for studies of membrane-spanning peptides; p. 126
23. Van der Wel PCA, Strandberg E, Killian JA, Koeppe RE II. Geometry and intrinsic tilt of a tryptophan-anchored transmembrane alpha-helix determined by ^{2}H NMR. Biophys J. 2002; 83:1479–1488. [PubMed: 12202373]
24. Dvinskikh SV, Castro V, Sandstrom D. Probing segmental order in lipid bilayers at variable hydration levels by amplitude- and phase-modulated cross-polarization NMR. Phys Chem. 2005; 7:3255–3257.
25. Koeppe RE II, Sun H, van der Wel PCA, Scherer EM, Pulay P, Greathouse DV. Combined Experimental/Theoretical Refinement of Indole Ring Geometry using Deuterium Magnetic Resonance and *ab initio* Calculations. J Am Chem Soc. 2003; 125:12268–12276. [PubMed: 14519012]
26. van der Wel PCA, Reed ND, Greathouse DV, Koeppe RE II. Orientation and motion of tryptophan interfacial anchors in membrane-spanning peptides. Biochemistry. 2007; 46:7514–7524. [PubMed: 17530863]
27. Koeppe RE II, Killian JA, Greathouse DV. Orientations of the tryptophan 9 and 11 side chains of the gramicidin channel based on deuterium NMR spectroscopy. Biophys J. 1994; 66:14–24. [PubMed: 7510525]
28. McKeone BJ, Pownall HJ, Massey JB. Ether phosphatidylcholines: Comparison of miscibility with ester phosphatidylcholines and sphingomyelin, vesicle fusion, and association with apolipoprotein A-1. Biochemistry. 1986; 25:7711–7716. [PubMed: 3099835]
29. Davis JH, Jeffrey KR, Valic MI, Bloom M, Higgs TP. Quadrupolar echo deuteron magnetic resonance spectroscopy in ordered hydrocarbon chains. Chem Phys Lett. 1976; 42:390–394.
30. Gall CM, DiVerdi JA, Opella SJ. Phenylalanine ring dynamics by solid-state 2H NMR. J Am Chem Soc. 1981; 103:5039–5043.
31. Killian JA, Taylor MJ, Koeppe RE II. Orientation of the valine-1 side chain of the gramicidin transmembrane channel and implications for channel functioning. A ^{2}H NMR study. Biochemistry. 1992; 31:11283–11290. [PubMed: 1280159]
32. Pulay P, Scherer EM, van der Wel PCA, Koeppe RE II. Importance of Tensor Asymmetry for the Analysis of ^{2}H NMR Spectra from Deuterated Aromatic Rings. J Am Chem Soc. 2005; 127:17488–17493. [PubMed: 16332101]
33. Greathouse DV, Hinton JF, Kim KS, Koeppe RE II. Gramicidin A/short-chain phospholipid dispersions: chain length dependence of gramicidin conformation and lipid organization. Biochemistry. 1994; 33:4291–4299. [PubMed: 7512381]

34. Turner GL, Hinton JF, Koeppe RE II, Parli JA, Millett FS. Difference in association of thallium(I) with gramicidin A and gramicidin B in trifluoroethanol determined by thallium-205 NMR. Biochim Biophys Acta. 1983; 756:133–137.
35. Bañó MC, Braco L, Abad C. New high-performance liquid chromatography-based methodology for monitoring the conformational transitions of self-associating hydrophobic peptides, incorporated into liposomes. J Chromatogr. 1988; 458:105–116. [PubMed: 2466865]
36. Andersen OS. Ion movement through gramicidin A channels. Single-channel measurements at very high potentials. Biophys J. 1983; 41:119–133. [PubMed: 6188500]
37. Sawyer DB, Koeppe RE II, Andersen OS. Gramicidin single-channel properties show no solvent-history dependence. Biophys J. 1990; 57:515–523. [PubMed: 1689593]
38. Sawyer DB, Koeppe RE II, Andersen OS. Induction of conductance heterogeneity in gramicidin channels. Biochemistry. 1989; 28:6571–6583. [PubMed: 2477060]
39. Durkin JT, Koeppe RE II, Andersen OS. Energetics of gramicidin hybrid channel formation as a test for structural equivalence. Side-chain substitutions in the native sequence. J Mol Biol. 1990; 211:221–234. [PubMed: 1688951]
40. Andersen OS, Bruno MJ, Sun H, Koeppe RE II. Single-molecule methods for monitoring changes in bilayer elastic properties. Methods in Molecular Biology. 2007; 400:541–568.
41. Durkin JT, Providence LL, Koeppe RE II, Andersen OS. Energetics of heterodimer formation among gramicidin analogues with an NH_2-terminal addition or deletion: Consequences of missing a residue at the join in the channel. J Mol Biol. 1993; 231:1102–1121. [PubMed: 7685829]
42. Mazet JL, Andersen OS, Koeppe RE II. Single-channel studies on linear gramicidins with altered amino acid sequences. A comparison of phenylalanine, tryptophan, and tyrosine substitutions at positions 1 and 11. Biophys J. 1984; 45:263–276. [PubMed: 6201199]
43. Russell EWB, Weiss LB, Navetta FI, Koeppe RE II, Andersen OS. Single-channel studies on linear gramicidins with altered amino acid side chains. Effects of altering the polarity of the side chain at position 1 in gramicidin A. Biophys J. 1986; 49:673–686. [PubMed: 2421794]
44. Becker MD, Koeppe RE II, Andersen OS. Amino acid substitutions and ion channel function. Model- dependent conclusions. Biophys J. 1992; 62:25–27. [PubMed: 1376168]
45. Urry DW. The gramicidin A transmembrane channel: a proposed π(L,D) helix. Proc Natl Acad Sci U S A. 1971; 68:672–676. [PubMed: 5276779]
46. Andersen OS, Apell H-J, Bamberg E, Busath DD, Koeppe RE II, Sigworth FJ, Szabo G, Urry DW, Woolley A. Gramicidin channel controversy — the structure in a lipid environment. Nature Struct Biol. 1999; 6:609. [PubMed: 10404209]
47. Veatch WR, Fossel ET, Blout ER. Conformation of gramicidin A. Biochemistry. 1974; 13:5249–5256. [PubMed: 4139971]
48. Langs DA. Three-dimensional structure at 0.86 Å of the uncomplexed form of the transmembrane ion channel peptide gramicidin A. Science. 1988; 241:188–191. [PubMed: 2455345]
49. Bouchard M, Benjamin DR, Tito P, Robinson CV, Dobson CM. Solvent effects on the conformation of the transmembrane peptide gramicidin A: insights from electrospray ionization mass spectrometry. Biophys J. 2000; 78:1010–1017. [PubMed: 10653814]
50. Burkhart BM, Li N, Langs DA, Pangborn WA, Duax WL. The conducting form of gramicidin A is a right-handed double-stranded double helix. Proc Natl Acad Sci U S A. 1998; 95:12950–12955. [PubMed: 9789021]
51. Andersen OS, Providence LL, Mattice GL, Koeppe RE II. Ion channels with L- and D-amino acids. Chemtracts: Biochemistry and Molecular Biology. 1997; 10:175–188.
52. Durrant JD, Caywood D, Busath DD. Tryptophan contributions to the empirical free-energy profile in gramicidin A/M heterodimer channels. Biophys J. 2006; 91:3230–3241. [PubMed: 16861266]
53. Mattice GL, Koeppe RE II, Providence LL, Andersen OS. Stabilizing effect of D-alanine-2 in gramicidin channels. Biochemistry. 1995; 34:6827–6837. [PubMed: 7538788]

Abbreviations

CD circular dichroism

DMPC	1,2-Dimyristoylphosphatidylcholine
DPhPC	1,2-Diphytanoylphosphatidylcholine
DMF	Dimethylformamide
DS	double stranded
gA	gramicidin A
MS	mass spectrometry
NMR	nuclear magnetic resonance
QCC	quadrupolar coupling constant
SEC	size exclusion chromatography
SS	single-stranded
TFA	trifluoroacetic acid

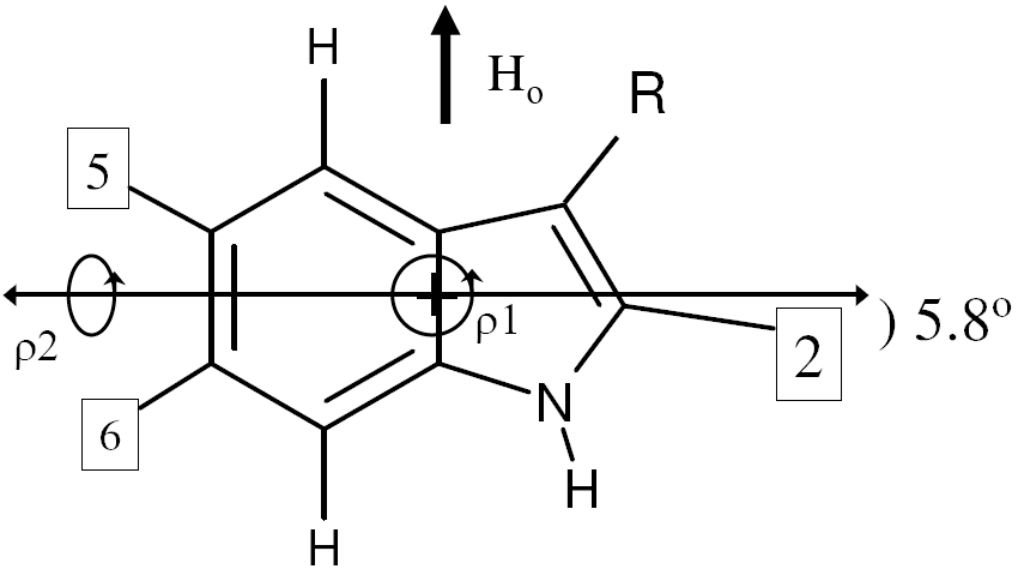

Figure 1.

Indole ring geometry and the rotational degrees of freedom, ρ_1 and ρ_2, for orienting the ring with respect to an external magnetic field. Ring positions 2, 5, and possibly 6 (numbered), become labeled—to different extents—by the $^1H/^2H$ exchange reaction described in Methods. The C2-H bond makes an angle of 5.8° with an axis that bisects the six-membered ring (25). Modified from reference (32).

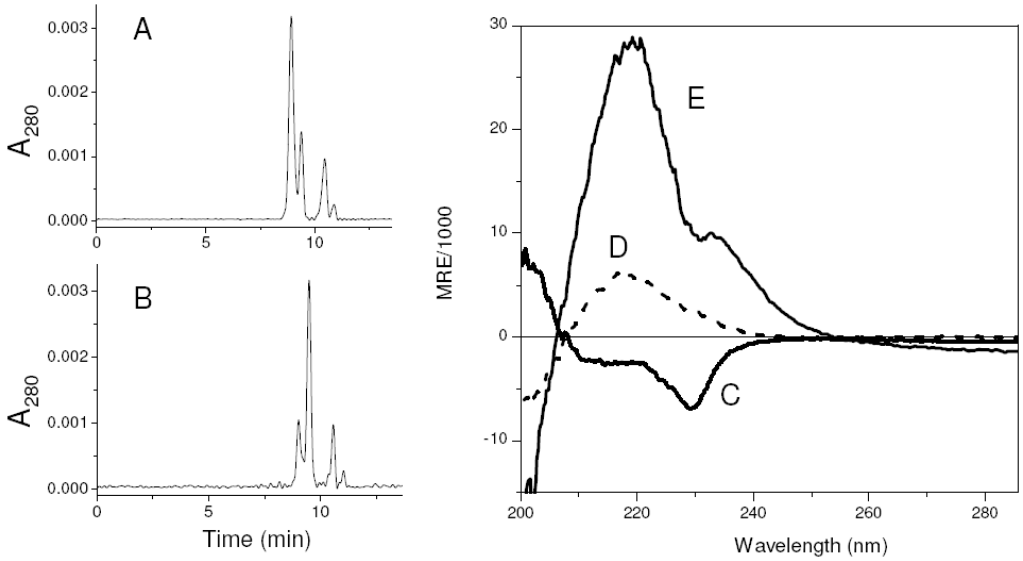

Figure 2.

Conformational analysis of the gA analogues using SEC analysis and CD spectroscopy. Left panels: SEC chromatograms indicate a preference for double-stranded conformers (~75%) for [Phe^{9,11}]gA (A), compared to ~75% single-stranded conformer for[Phe^{13,15}]gA (B). The first two peaks, eluting at about 9.0 and 9.5 min represent the DS and SS conformers, respectively. (The peaks eluting later than 10 min represent changes in refractive index when lipids elute.) Right panel: CD spectra for: C, [Phe^{9,11}]gA; D, [Phe^{13,15}]gA; and E. native gA. DMPC, 1/50 (gramicidin/lipid molar ratio), 25 °C.

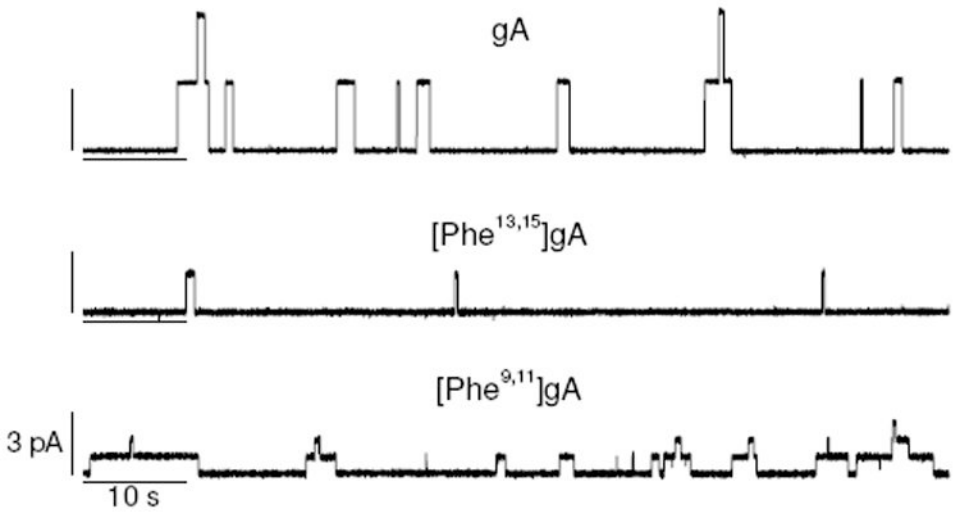

Figure 3.

Single-channel current traces for channels formed by the native gA and the sequence-substituted [Phe^{13,15}]gA and [Phe^{9,11}]gA analogues. DPhPC, 1 M NaCl, 200 mV, 25 °C. The labels on the bottom calibration bars apply also to the calibration bars in the top two traces.

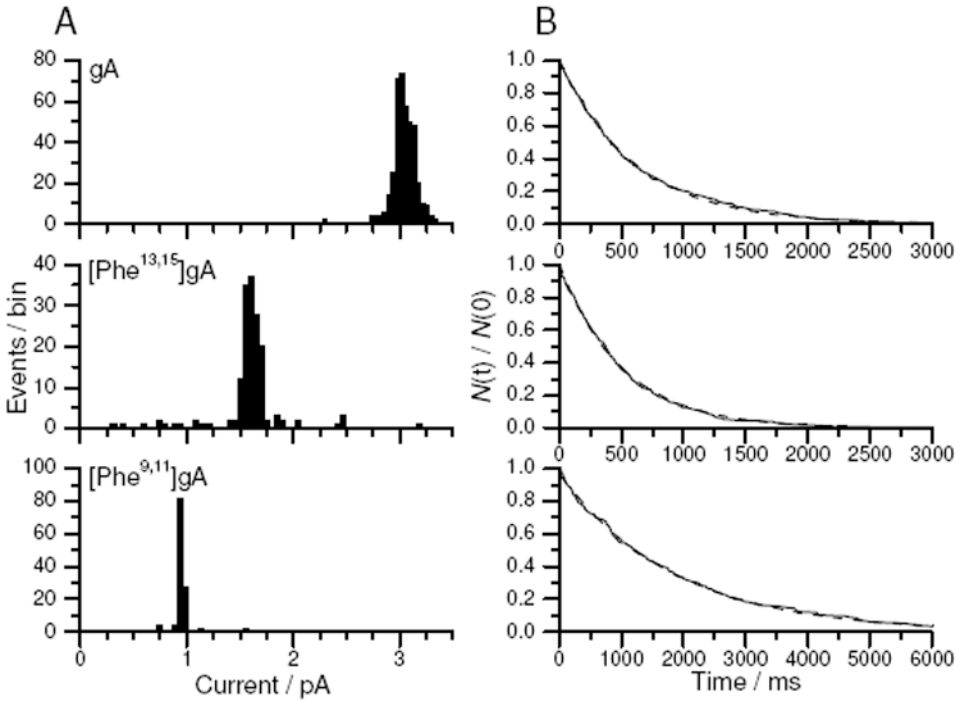

Figure 4.

Single-channel amplitude and lifetime distributions for channels formed by the native gA and the sequence-substituted [Phe^{13,15}]gA and [Phe^{9,11}]gA analogues. A) Amplitude histograms for, from top to bottom: gA channels; [Phe^{13,15}]gA channels; and [Phe^{9,11}]gA channels. B) Lifetime distributions, plotted as normalized survivor histograms for, from top to bottom: gA channels; [Phe^{13,15}]gA channels; and [Phe^{9,11}]gA channels. The solid curve denotes the normalized survivor distribution, the interrupted curve denotes the fit of a single exponential distribution to the results. DPhPC, 1 M NaCl, 200 mV, 25 °C.

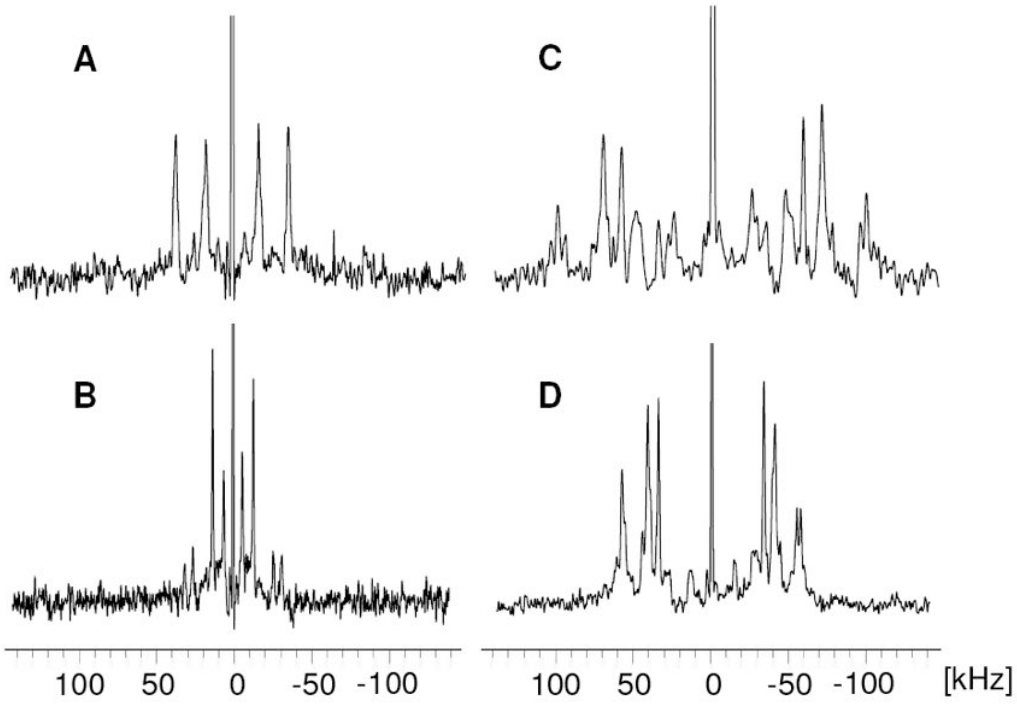

Figure 5.

^{2}H NMR spectra of doubly-substituted Trp→Phe gA analogues in oriented DMPC multilayers: A and B, [Phe^{13,15}]gA oriented β = 0° and β = 90°, respectively. C and D, [Phe^{9,11}]gA oriented at β = 0 and. β = 90°, respectively. Temperature: 50 °C.

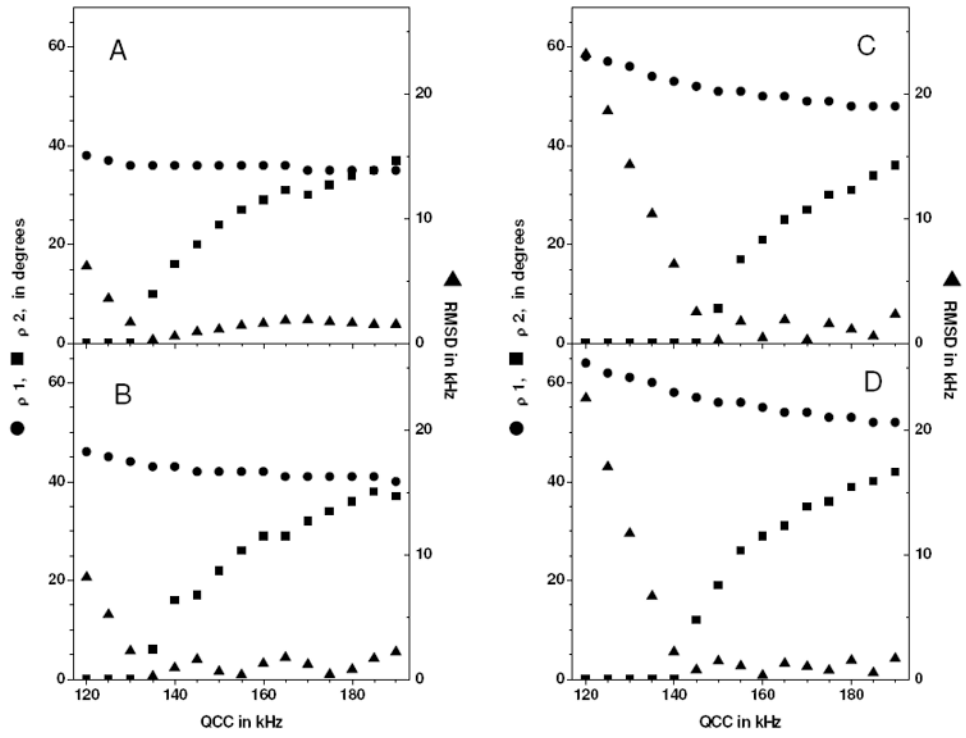

Figure 6.

Variation of the best-fit ρ1 (●), ρ2 (■) and corresponding RMSD (▲), as functions of apparent QCC for the indole rings of: A. Trp^{9} in [$Phe^{13,15}$]gA; B. Trp^{11} in [$Phe^{13,15}$]gA; C. Trp^{13} in [$Phe^{9,11}$]gA; D. Trp^{15} in [$Phe^{9,11}$]gA.

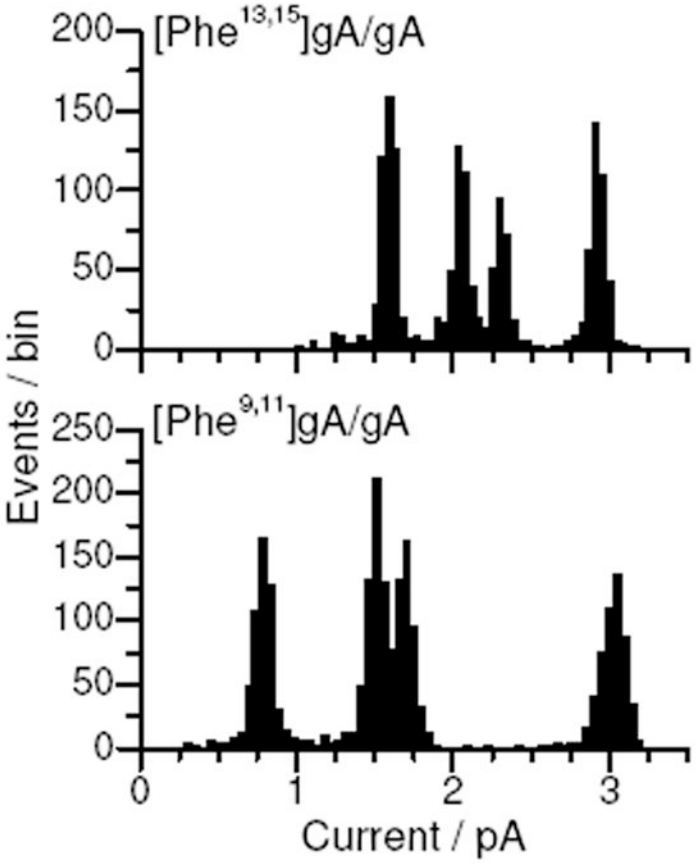

Figure 7.

Heterodimer formation experiment with [Phe^{9,11}]gA and native gA, or [Phe^{13,15}]gA, and native gA, added to both sides of a bilayer. Top: Single-channel current transition amplitude histogram with [Phe^{13,15}]gA, and native gA; in addition to the two peaks representing the two homodimeric [Phe^{13,15}]gA/[Phe^{13,15}]gA and gA/gA and channels, there are two new peaks with intermediate current transition amplitudes, which represent the gA/[Phe^{13,15}]gA and [Phe^{13,15}]gA/gA heterodimeric channels. The orientation of the two peaks, relative to the applied potential is identified in Fig. 8. (The current transitions amplitude histograms are based on the cumulative results of individual experiments each obtained using three to ten different “small” membranes isolated from the large bilayer using the bilayer punch. The individual histograms obtained from each small membrane displayed a similar distribution as the cumulative histograms.) The relative heterodimer appearance rate (Eq. 1) is 0.73; based on the lifetime distributions (not shown), the relative heterodimer lifetime (Eq. 2) is 1.03. Bottom: Single-channel current transition amplitude histogram with [Phe^{9,11}]gA, and native gA; in addition to the two peaks representing the two homodimeric [Phe^{9,11}]gA/[Phe^{9,11}]gA and gA/gA channels, there are two new peaks with intermediate current transition amplitudes, which represent the gA/[Phe^{9,11}]gA and [Phe^{9,11}]gA/gA heterodimeric channels. The orientation of the two peaks, relative to the applied potential is identified in Fig. 8. The relative heterodimer appearance rate (Eq. 1) is 1.02; based on the lifetime distributions (not shown), the relative heterodimer lifetime (Eq. 2) is 0.96. DPhPC, 1 M NaCl, 200 mV, 25 °C.

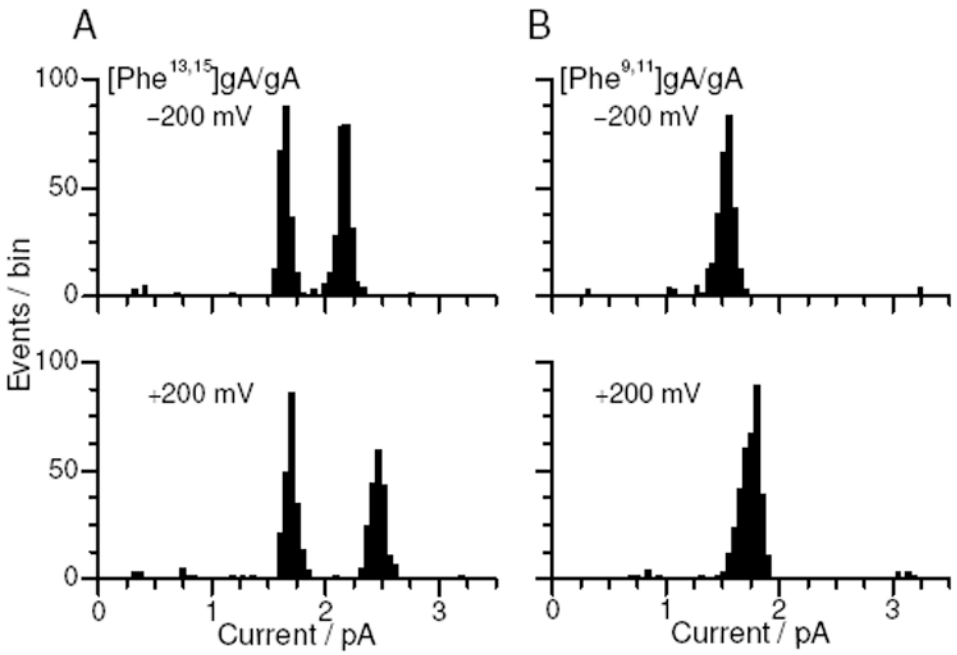

Figure 8.

Orientation of the heterodimeric channels underlying the two heterodimer peaks in the current transition amplitude histograms in Fig 7. Left: results for [Phe^{13,15}]gA/gA, where [Phe^{13,15}]gA is added only to the *cis* compartment (the electrical reference) and the native gA is added only to the *trans* compartment. [Phe^{13,15}]gA is able to cross the bilayer and form single-stranded cation-conducting channels, whereas gA is not, as evident from the presence of a peak representing the symmetric [Phe^{13,15}]gA homodimeric channels (at ~1.7 pA) with no corresponding peak representing the symmetric gA homodimeric channels. In the recordings at −200 mV (when the current is toward the gA-containing chamber), the heterodimeric peak is at ~2.2 pA; in the recordings at +200 mV (when the current is from the gA-containing chamber), the heterodimeric peak is at ~2.4 pA. Right: results for [Phe^{9,11}]gA/gA, where [Phe^{9,11}]gA is added only to the *cis* compartment (the electrical reference) and the native gA is added only to the *trans* chamber. In this case, we observe neither of the symmetric, homodimeric channel types. In the recordings at −200 mV (when the current is toward the gA-containing chamber), the most prominent heterodimeric peak is the peak at ~1.6 pA; in the recordings at +200 mV (when the current is from the gA-containing chamber), the most prominent heterodimeric peak is the peak at ~1.8 pA.

Table 1

Single-channel properties of Trp→Phe-substituted gA analogues[a]

Analogue	*g* ± SD (pS)[b]	τ(ms)[f]	
native gA	15.0 ± 0.2[c]	600 ± 50[c]	840[d]
[Phe^{9}]gA	6.0 ± 0.1[d]		1000[d]
[Phe^{11}]gA	8.7 ± 0.3[d]		2300[d]
[Phe^{13}]gA	11.2 ± 0.2[d]		800[d]
[Phe^{15}]gA	10.9 ± 0.2[d]		800[d]
[Phe^{9,11}] gA	3.9 ± 0.1[c]	1850 ± 100[c]	
[Phe^{13,15}]gA	7.9 ± 0.2[c]	500 ± 50[c]	
[Phe^{9,15}]gA	4.1 ± 0.1[d]		750[d]
[Phe^{9,11,13}]gA	2.1 ± 0.1[d]		2300[d]
[Phe^{9,13,15}]gA	3.0 ± 0.5[d]		5[d]
[Phe^{11,13,15}]gA	3.4 ± 0.1[d]		2100[d]
[Phe^{9,11,13,15}]gA	8.0 ± 0.5[e]		330[e]

[a] DPhPC, 1 M NaCl, 200 mV, 25 °C.

[b] Based on 2 – 4 individual experiments, with 1,000 – 2,000 single-channel current transitions for each channel type.

[c] Results from this study.

[d] Results from (7).

[e] Results obtained in 1.0 M CsCl, from (4). For comparison, *g* for gA is 47 ± 1 ps. The single-channel lifetimes of gA channels in 1.0 M NaCl and CsCl are similar (53).

[f] Based on 500 – 1,000 single-channel events; except where noted, the uncertainty is about 10%. The single-channel lifetimes in DPhPC/*n*-decane bilayers have varied over the years, depending in part on the source of the phytanic acid. We therefore list separately the results from this study and those from Becker et al. (7).

Table 2

^{2}H quadrupolar splittings and assignments for Trp rings in Phe-substituted gramicidin A analogues, oriented at β = 0° in DMPC

Sequence position	Ring position	[Phe^{9,11}]gA ($\Delta\nu_q$, in kHz)	[Phe^{13,15}]gA ($\Delta\nu_q$, in kHz)	gA[a] ($\Delta\nu_q$, in kHz)
9	2		33	43
11	2		71	96
13	2	124		106
15	2	150		125
9	5		142	151
11	5		170	188
13	5	211		205
15	5	211		205

[a] Data from Koeppe et al. (25).

Table 3

Single-channel conductances and lifetimes of heterodimeric channels formed between [Phe^{9,11}]gA or [Phe^{13,15}]gA and gA.

[Phe^{9,11}]gA/gA heterodimers	***g* ± SD^{a} (pS)**	**τ^{a} (ms)**
gA→gA	15.0 ± 0.3	580
gA→[Phe^{9,11}]gA	8.4 ± 0.1	1000
[Phe^{9,11}]gA→gA	7.5 ± 0.2	920
[Phe^{9,11}]gA→[Phe^{9,11}]gA	3.9 ± 0.1	1850
[Phe^{13,15}]gA/gA heterodimers		
gA→gA	14.7 ± 0.2	640
gA→[Phe^{13,15}]gA	11.5 ± 0.2	560
[Phe^{13,15}]gA→gA	10.2 ± 0.2	610
[Phe^{13,15}]gA→[Phe^{13,15}]gA	7.9 ± 0.2	500

^{a}Results from 2 – 3 independent experiments done with symmetric addition of gA and the Trp→Phe –substituted gA analogue to both sides of the membrane, cf. Fig. 7, each with 3 – 10 small membranes isolated using the bilayer punch. The orientation of the heterodimeric channels was determined from the results in Figure 8. The uncertainty in the single-channel lifetimes is about 10%